ISSN 0747-9239, Seismic Instruments, 2018, Vol. 54, No. 4, pp. 461–478. © Allerton Press, Inc., 2018.
Original Russian Text © Tuo Shen, E.A. Rogozhin, 2017, published in Voprosy Inzhenernoi Seismologii, 2017, Vol. 44, No. 4, pp. 29–50.

Geodynamic and Seismotectonic Activity in Eastern Tibet in the 21st Century

Tuo Shen[a], * and E. A. Rogozhin[a], **

[a]*Schmidt Institute of Physics of the Earth, Russian Academy of Sciences, Moscow, 123242 Russia*

**e-mail: 283473562@qq.com*

***e-mail: eurog@ifz.ru*

Abstract—At the beginning of the 21st century, a series of great earthquakes were recorded in northeastern Tibet, along the periphery of the Bayan Hara lithospheric block. An earthquake with M_S = 8.1 occurred within the East Kunlun fault zone in the Kunlun Mountains, which caused an extended surface rupture with left-lateral strike slip. An earthquake with M_S = 8 occurred in Wenchuan (China) on May 12, 2008, giving rise to an extended overthrust along the Lunmanshan fault zone. An earthquake with M_S = 7.1 occurred in Yushu (China) on April 14, 2010; its epicenter was on the Grazze–Yushu–Funchuoshan fault; a left-lateral strike-slip offset was observed on the surface. An earthquake with M_S = 7 occurred in the vicinity of Lushan on April 20, 2013; its epicenter was within the Lunmanshan fault zone, 103 km southwest of the zone of the catastrophic Wenchuan earthquake. An earthquake with M_S = 8.2 occurred in Nepal on April 25, 2015. Based on the CSN seismic catalog, the energy of all earthquakes in eastern Tibet at the end of the 20th and beginning of the 21st centuries was estimated. It was found that Tibet was seismically quiet from 1980 to 2000. The beginning of the 21st century has been marked by seismic activation with earthquake sources migrating southward to surround the Bayan Hara lithospheric block from every quarter. Therefore, this block can be regarded as one of the most seismically active regions of China.

Keywords: Bayan Hara block, Himalayas, northeastern Tibet, epicenter, earthquake, migration, seismic rupture

DOI: 10.3103/S0747923918040084

INTRODUCTION

The Tibetan Plateau is located to the south of the Tien Shan Mountains and Tarim Basin, to the north of the Himalayan fold mountains, and to the west of the Chang Jiang River. As a result of collision of the Hindustani and Eurasian plates and active uplift of the Tien Shan and Himalayas, the Tibetan Plateau has been squeezed against the crustal blocks that surround it, stretching in a nearly east-west direction (Dewey, 2005). In terms of modern geodynamics and seismotectonics, the Tibetan Plateau can be divided into four subregions: the Central Tibetan Plateau, the Himalayan collisional orogenic belt, the transitional orogenic belt of the Tien Shan and the Tarim, and the ancient Yangtze Plate bordering the Tibetan Plateau in the east.

The Bayan Hara block belongs to the Central Tibetan Plateau. The block exhibits no significant young deformations. According to GPS measurements, the block is moving eastward (Xu Zhiqin et al., 2011). The Bayan Hara tectonic block is bounded by the East Kunlun fault in the north, the Xianshui–Yushu fault zone in the south, and the Lumen Shan Fault in the east. The East Kunlun left-lateral strike-slip fault striking nearly EW exhibits a displacement rate of more than 10 mm/year. The walls of the WNW-trending left-lateral strike-slip Xianshuihe–Yushu fault also move at a rate of 10 mm/year. The East Kunlun, Xianshui–Yushu, and Lumen Shan faults bound the Bayan Hara block, which that has become the most seismically active territory of China in the 21st century (Deng Qidong et al., 2010; Xu Zhiqin et al., 2011).

At the beginning of the 21st century, the four strongest earthquakes with magnitudes greater than 7 (M_S) occurred in northeastern Tibet, at the periphery of the Bayan Hara tectonic block (Fig. 1). An earthquake with M_S = 8.1 occurred in the East Kunlun fault zone on October 14, 2001. This earthquake was the first with a magnitude of over 8 in China in the 21st century. The focal mechanism of the earthquake was left-lateral strike slip. An earthquake with M_S = 8 occurred in the southeastern part of Wenchuan County. The epicenter of the earthquake was confined to the Longmenshan fault zone. The strain in the source region was due to thrust motion. The earthquake hypocenter was at a depth of 14 km. An earthquake with M_S = 7.1 occurred in the Yushu district of the Tibet Autonomous Region of Qinghai Province on April 14, 2010.

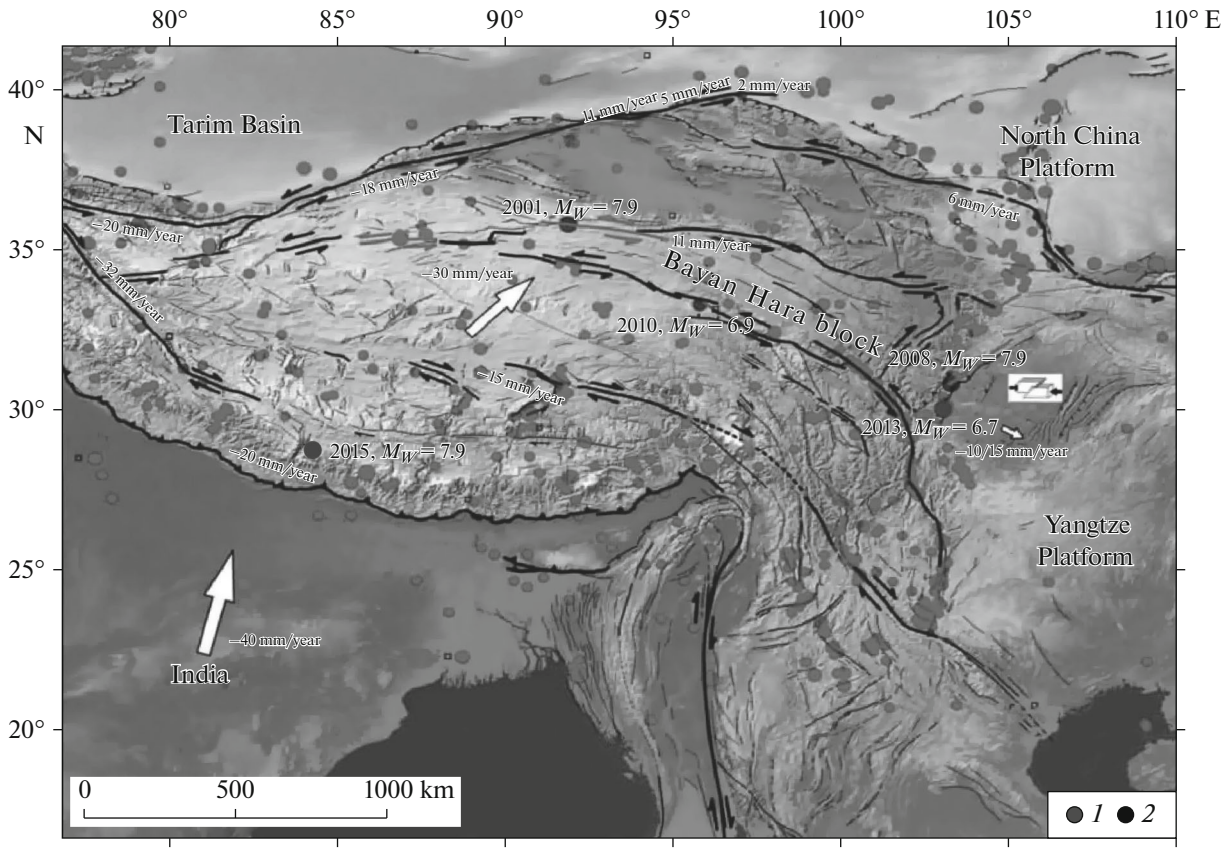

Fig. 1. Epicenters of strong earthquakes in Tibet and Himalayas (*1*) and strongest seismic events at margins of Bayan Hara block (after (Xu Xiwei et al., 2013)) and in Nepal (*2*).

The epicenter of the earthquake was near the Grazze–Yushu–Funchuoshan fault. The strain in the source region was due to left-lateral strike-slip motion. The hypocenter was at a depth of 33 km. An earthquake with M_S = 7 occurred in the vicinity of Lushan on April 20, 2013; its epicenter was confined to the Lunmanshan fault zone. The earthquake hypocenter was at a depth of 14 km. The earthquake source region was 103 km southwest of the 2008 Wenchuan earthquake zone. More than 1.5 mln inhabitants of Sichuan Province were affected by the earthquake. Across a vast territory, buildings and structures in small towns and villages were destroyed or damaged.

Moreover, a catastrophic earthquake occurred in the Himalayas, in Gorkha, on April 25, 2015. Estimated from Quick CMT, the moment magnitude of the earthquake was M_W = 7.9. The instrumental epicenter was in Nepal, 75 km northwest of Kathmandu. The hypocenter was at a depth of 13 km. The active plane in the earthquake source region formed in the zone of the gently northward-dipping Main Central Thrust in the Himalayas (Valdiya, 1980, 1988; Gansser, 1982; Chandra, 1992; Pandey et al., 1999). The thrust separates the High and Low Himalayan tectonic zones located to the north and south of the thrust, respectively.

The above examples show that the beginning of the 21st century is characterized by increased seismic activity in eastern Tibet and the Himalayas (Nepal).

There has been considerable discussion in the scientific literature as to the time dependence of the seismic process. For instance, global seismicity from 1900 to 1999 is analyzed in (Engdahl and Villaseñor, 2002), which presents a fairly complete world catalog of earthquakes in the 20th century and some results of its analysis. It is observed that seismic activity is a time-dependent phenomenon; therefore, seismic moment release is characterized by considerable fluctuations. Time-dependent clustering of large earthquakes, as well as a time-dependent global distribution of earthquakes, is discussed in (Lombardi and Marzocchi, 2007). It can be therefore stated that seismicity probably has some quasi-periodicity. It is stated in (Lutikov and Rogozhin, 2014) that the beginning of the 21st century has been marked by an increase in earthquake activity worldwide. As shown above, the phenomenon of strong earthquakes in Tibet agrees with the worldwide trend in seismic activity.

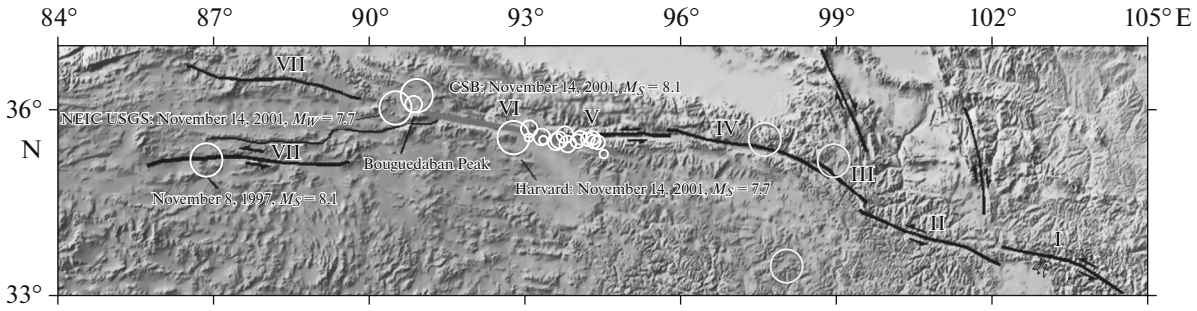

Fig. 2. Seismic rupture and epicenters of main shock and strongest aftershocks of 2001 East Kunlun earthquake with M = 8.1, data from different sources.

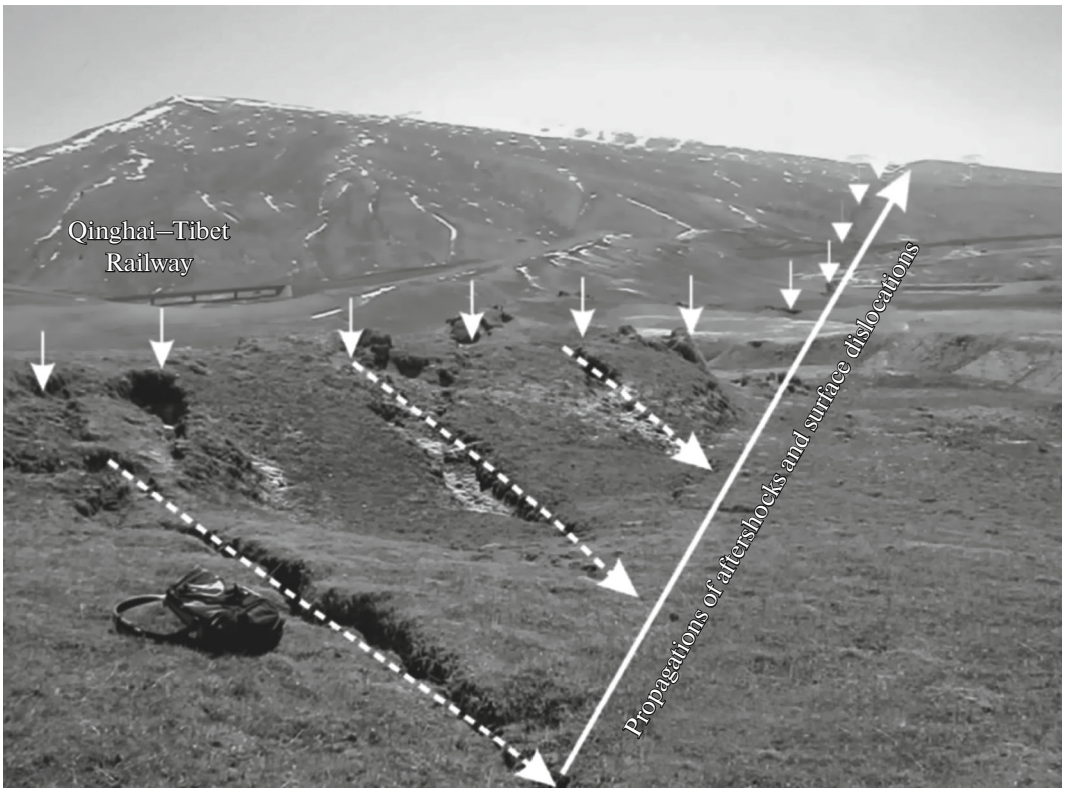

Fig. 3. En echelon surface fractures generated by 2001 East Kunlun earthquake (Li Dewei, 2010): view looking east.

TECTONIC POSITION AND GEOLOGICAL MANIFESTATIONS OF THE LARGEST EARTHQUAKES IN EASTERN TIBET AND THE HIMALAYAS OF NEPAL IN THE 21ST CENTURY

Kunlun Earthquake in 2001

An earthquake with a magnitude of 8.1 occurred in Qinghai Province on November 14, 2001. The source was on the active Kunlun fault (Van der Word et al., 2003). The epicenter coordinates were 36.1° N, 90.9° E; the hypocenter was at a depth of 10 km. This earthquake was the first with a magnitude of over 8 in China in the 21st century. The earthquake produced a 400-km-long surface rupture along the Khokh Sai Hu fault (a segment of the Kunlun deep fault). The average amount of displacement along this fault is 11–16 mm/year. The kinematics of seismogenic displacement is left-lateral strike slip (Figs. 2–6).

The earthquake occurred in the eastern part of the Kunlun orogenic uplift. Primary (seismotectonic) and secondary (gravitational and vibrational) surface dislocations are observed within a strip a few km wide and about 400 km long. The surface rupture is represented by en echelon left-lateral strike slips with some segments trending in a west-northwestern direction (270°–290°). Rupture cracks are oriented in the east-

Fig. 4. Seismic rupture caused by 2001 Kunlun earthquake. Photo by Jun Shen.

Fig. 5. Road damage caused by 2001 Kunlun earthquake. Photo by Jun Shen.

northeastern and northeastern directions (80°–85°, Riedel megashear R, and 35°–45°, Riedel R' megashear, respectively). The horizontal displacement is from 1 to 2 m. The focal mechanism solution determined from the catalog of the National Earthquake Information Center of the US Geological Survey (NEIC USGS) (Fig. 6) shows that the nearly north-south trending nodal plane dips steeply and the earthquake source region is dominated by right-lateral strike-slip motions due to compression and tension stresses. The second nodal plane trends near west-east and dips steeply southward. This plane, along which compression and tension stresses are oriented in the northeastern and northwestern directions, respectively, is characterized by left-lateral strike-slip displacement. It is this plane that should be regarded as an active faulting plane, since left-lateral strike-slip displacements are observed on surface ruptures (Figs. 4–6). An elongated cluster of the strongest aftershocks is oriented in the same direction (Fig. 3).

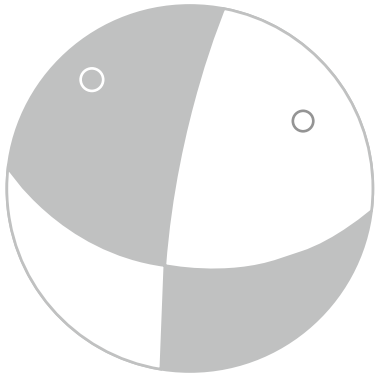

Fig. 6. Focal mechanism of November 14, 2001, Kunlun earthquake (NEIC USGS data).

Wenchuan Earthquake in 2008

A catastrophic earthquake with a magnitude of 8.0, called the 5.12 Wenchuan earthquake, occurred in China on May 12, 2008, in Sichuan province, between the Sinian Mountains of Tibet and the Sichuan depression. The instrumental epicenter was in the southeast part of Wenchuan County. The depth of the earthquake hypocenter was 14 km. This earthquake, one of the most massive and devastating in China, caused heavy casualties and large-scale destruction of buildings and infrastructure. Many counties, cities, and villages were damaged as a result of the main shock and aftershocks. Sichuan province was most affected. The maximum intensity of the quake was XI on the Chinese macroseismic scale. As the rupture front moved from the southern part of Wenchuan County to Qingchuan, a northeast-trending system of surface ruptures formed, the total length of which reaches 240 km, confined to the Longmanshan fault zone. Seismic ruptures broke the surface and destroyed or damaged buildings, houses, bridges, roads (Figs. 7 to 9), etc., as a result of right-lateral strike-slip (1.5–2.5 m) and thrust (2–5 m) motions. The earthquake also caused tens of thousands of landslides, rockslides, and debris streams. Landslips and rockslides gave rise to dozens of lakes. In other words, geological effects turned out to be the most destructive factor.

A retrospective analysis of seismicity variations in the vast region of eastern Tibet showed that the Wenchuan earthquake zone was characterized by abnormally low seismicity in the 1970s–1990s: there were few earthquakes with $M \geq 5.0$ since the 1980s, few earthquakes with $M \geq 7.0$ since the early 1990s, and few earthquakes with $M \geq 7.8$ since the early 1970s. While there have been moderate earthquakes ($4.0 \geq M \geq 5.9$) and swarm sequences of weak shocks since the beginning of the 21st century, the source region has been like a seismic gap (Yan Xue et al., 2009). GPS-measured horizontal deformations on the surface in China show that the source region was characterized by abnormally low motion rates prior to earthquakes in 1999–2007. Apparently, this was due to accumulation of stresses in the Earth's crust (Wang et al., 2008; Guohua Gu et al., 2009).

A number of studies were carried out in the earthquake zone in summer and autumn 2008, including a seismotectonic study, mapping of seismic dislocations, a macroseismic survey of buildings and structures, recording of aftershocks by a network of temporary and permanent seismic stations, trenching across the surface rupture zone, and geodetic and remote seismic observations (Burchfiel et al., 2008; Chen Yun-tai et al., 2008; Ran et al., 2008; Xu et al., 2008; Fu et al., 2009). The findings of the studies were promptly published. Therefore, the earthquake can be considered very well studied.

The two most extended, nearly parallel branches have been distinguished: the northwestern branch 240 km long along the Yingxiu–Beichuan fault and a 70-km-long southeastern branch running along the Guangxian–Anxian fault. The distance between them varies from 5 to 11 km. There are also inferior seismic rupture zones trending northeast and northwest.

A seismic network deployed in Sichuan province recorded 33216 aftershocks after the main shock on October 11, 2008. Among them, there were 228 aftershocks with magnitudes of 4.0–4.9, 32 aftershocks with magnitudes of 5.0–5.9, and 8 shocks with magnitudes of 6.0–6.4. The aftershock epicenters were clustered near the Longmanshan fault zone, within a narrow strip extending more than 300 km (http://earthquakes.usgs.gov). The aftershock epicenters remained confined to a narrow seismic rupture zone within a month of the main shock.

Figure 10 shows the focal mechanism solution for the earthquake on May 12, 2008, computed by the centroid moment tensor method in NEIC USGS. It

Fig. 7. Gently sloping scarp caused by 2008 Wenchuan earthquake, courtyard of Sino-French secondary school, Bailu.

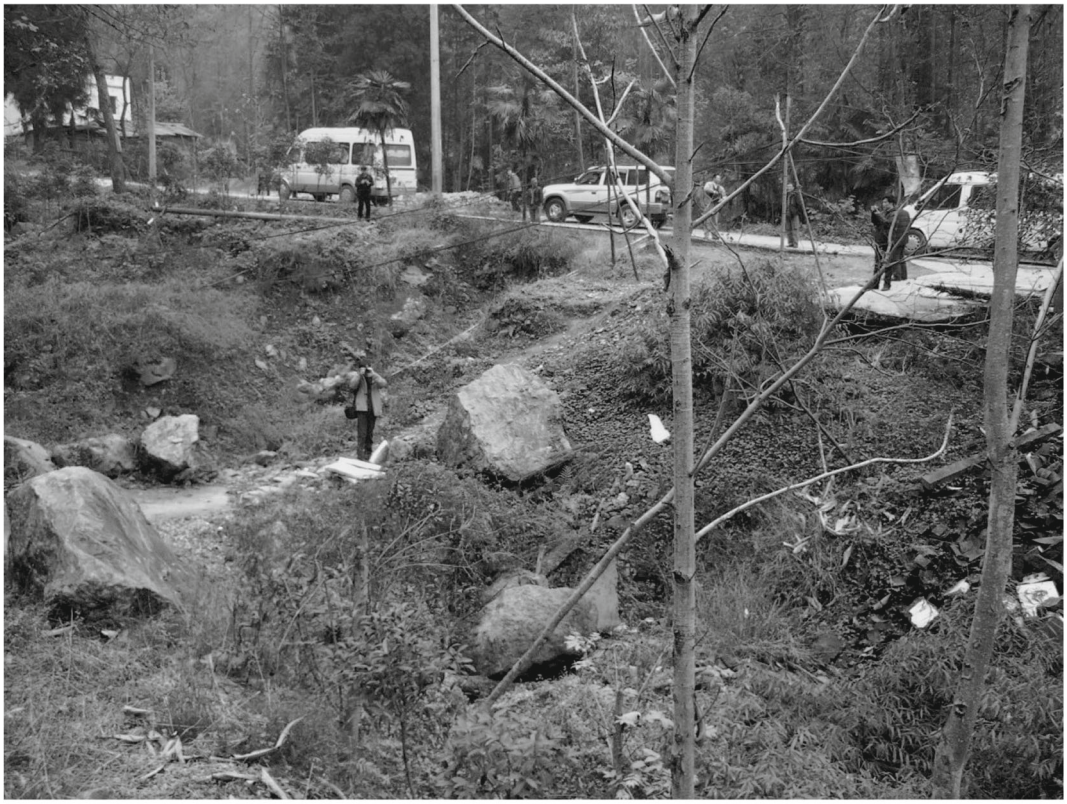

Fig. 8. Scarp generated by 2008 Wenchuan earthquake, vicinity of village of Hongkou. People with cameras are standing on sections of concrete road shifted by right-lateral strike slip and thrust motions.

Fig. 9. Ruins of house in village of Hongkou after 2008 Wenchuan earthquake. Right-lateral strike-slip shifted back wall of house at foot of seismogenic scarp.

indicates that the earthquake generation process was due to prevailing NW-oriented compressive stresses. One nodal plane (NP1) was a gently dipping (DP = 23°) plane striking northeast; the other plane (NP2) was a steep one (DP = 67°) trending northeast. The gently dipping plane exhibits thrust motion with a left-lateral strike-slip component. On the steeply dipping plane, displacement is due to thrust motion (the northeast wall is uplifted) and right-lateral strike-slip motion. Taking into account the nature of the displacements observed along primary surface ruptures, it is the steeply dipping, northwest-trending plane (NP2) that should be regarded as active plane in the earthquake source region.

It is known that any earthquake-proof building located within a rupture zone (X–XI-point seismicity) is doomed to complete destruction, even if the shaking intensity and ground acceleration are relatively small. This is confirmed by the above examples concerning the May 12, 2008, Wenchuan earthquake. The buildings located at the Ying Xiu seismic station and nearby were completely destroyed by surface fault ruptures; however, the recorded ground acceleration was just 205 cm/s^2 (7–8 points on the Chinese seismic intensity scale).

Lushan Earthquake of 2013

A devastating earthquake with a magnitude of $M = 7$ occurred in China on April 20, 2013. The epicenter coordinates were 30.29° N and 103.03° E (Fig. 11). The earthquake source was in Sichuan province at a depth of 20 km, 105 km west-southwest of Chengdu. Figure 11 also shows the epicenters of aftershocks during the first day.

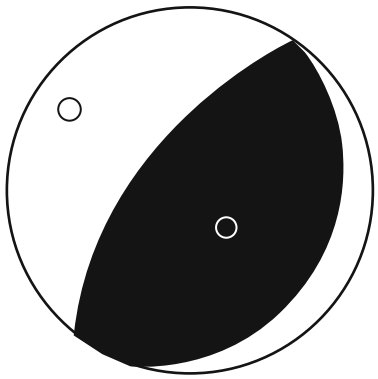

Fig. 10. Focal mechanism solution for main shock of Wenchuan earthquake, NEIC USGS data.

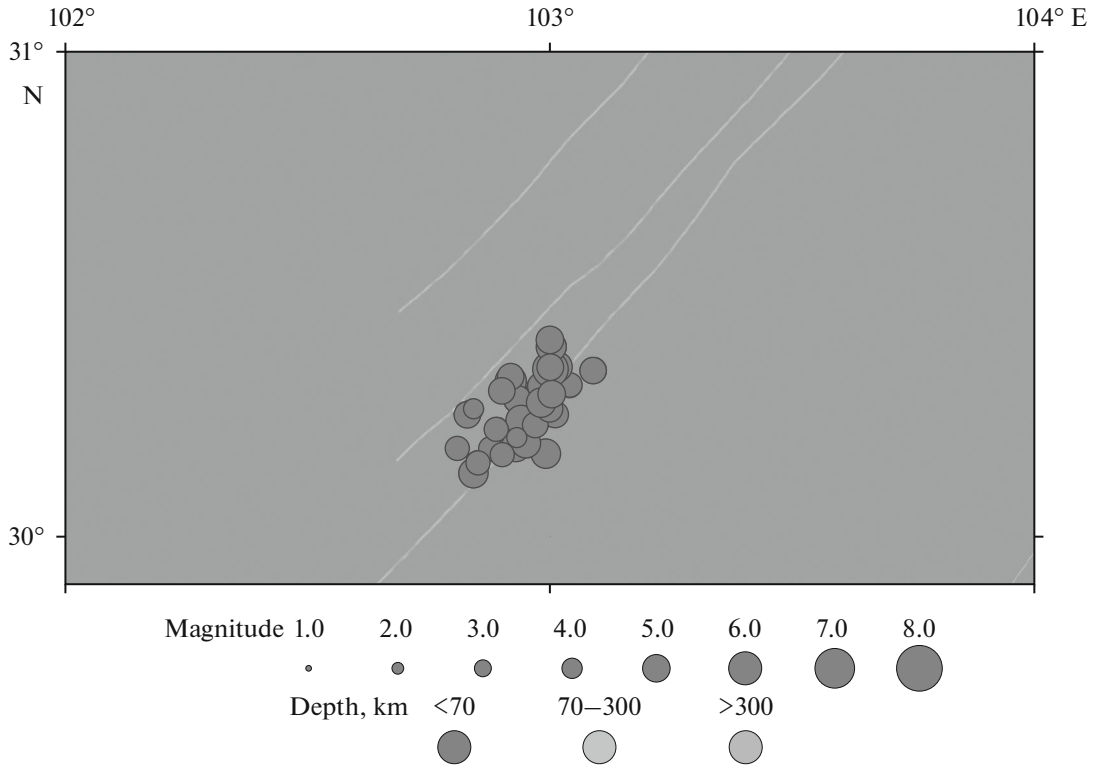

Fig. 11. Epicenters of main shock and aftershocks of April 20, 2014 Lushan earthquake: April 20–22, 2013 (Sobisevich et al., 2017). Lines show faults of Longmenshan fault system.

This quake is called the Lushan earthquake. The epicenter was located 103 km southwest of the zone of the catastrophic $M = 8$ Wenchuan earthquake on May 12, 2008. The China Earthquake Networks Center (CTNC) recorded more than 30 aftershocks with $M = 3.0–5.0$ on April 20–22, 2013. Their epicenters were within a compact linear cluster about 50 km long and 15 km wide, confined to the Longmenshan active fault zone (Fig. 1). The aftershocks of the Lushan earthquake "increased" the epicentral area of aftershocks of the May 12, 2008 Wenchuan earthquake in the southwest direction (Sobisevich et al., 2017).

The Lushan earthquake caused 208 fatalities, and over 11800 people were injured. Over 1.5 mln inhabitants of Sichuan province were affected by the earthquake. Buildings and structures were destroyed and damaged in small towns and villages across a vast territory. The intensity at the epicenter was from 8.5 to 9 points.

The major axes of oval-shaped isoseismals 5–8 extend in a southwest-to-northeast direction. In two large towns, Linqiong with a population of 56000 and Chengdu with a population of about 4 mln, the earthquake resulted in shaking felt as 6-point and 5-point earthquakes, respectively.

The epicenter of this seismic event was confined to the Shuangshi–Dachuan fault (Fig. 11), which is part of the Longmenshan active fault zone, over 500 km long. This fault zone separates the Paleozoic uplift of the Sinian Mountains in the northwest (on the eastern margin of the Tibetan Plateau) and the Sichuan Basin at the southeast wall of the fault zone. The earthquake source region was at the southwestern end of this fault zone. The fault strands of this disjunctive zone are thrusts with a right-lateral strike-slip component, dipping northwest, beneath the Sinian mountains. The fault zone is expressed topographically as a system of diagonally oriented ridges in the foothills.

Primary seismic dislocations of the 2013 earthquake were discovered in very small areas (Figs. 12a–12c). En echelon systems of gap fractures indicate that there was right-lateral motion along rupture segments. These fractures and belts of liquefaction structures extend for several tens of kilometers in the vicinity of the villages of Dachuan, Shuangshi, and Dasi. One fracture was exposed by a trench (Fig. 12d). It was observed in the trench that a rupture dipping northwestward at an angle of 75° reaches the surface. Within the epicentral zone, numerous landslides and rock falls occurred on the steep slopes of valleys crossing ridges in the foothills. Large stones blocked the roads in many places. Extensive seismogravitational dislocations were also typical of the 2008 earthquake.

The focal mechanism of the April 20, 2013, earthquake was determined by the Geophysical Service, Russian Academy of Sciences (GS RAS), from the

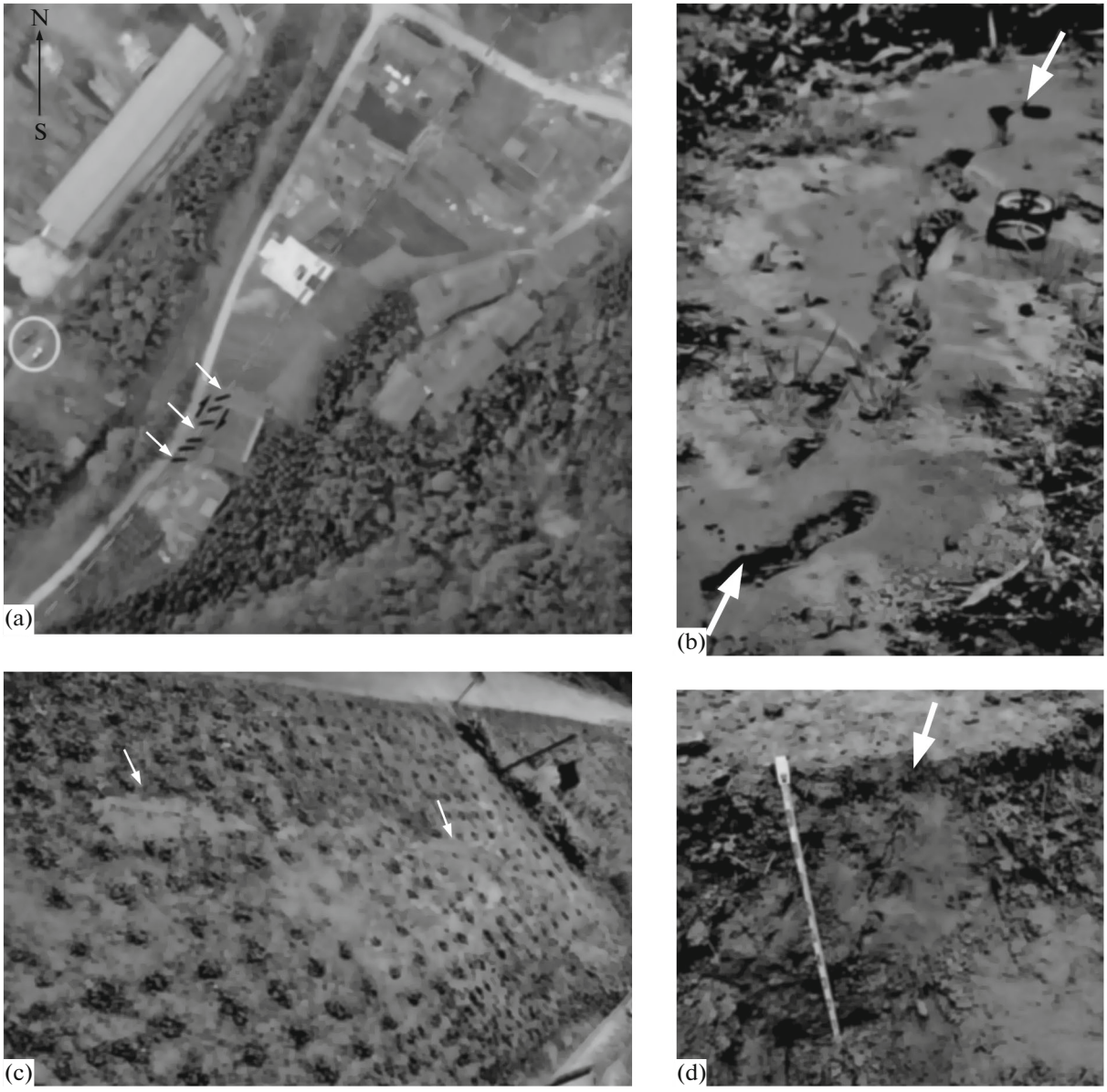

Fig. 12. Dislocations caused by 2013 Lushan earthquake: en echelon surface fractures and liquefaction of soils. (a) High-precision aerial photography did not reveal any lengthy seismic surface rupture zones (Shuangshi region); arrows indicate en echelon surface fractures; panels (b) and (c) show fractures with sand boils (striking north-northeast); (d) fracture exposed on wall of trench.

first arrivals of longitudinal waves at 217 stations. The focal mechanism is shown in Fig. 13 as a lower-hemisphere stereographic projection. The earthquake was due to high compressive stresses oriented in a northwestern direction. Tension forces acted in a near-vertical direction.

Both nodal planes trend in a northeast-southwest direction. One nodal plane is rather steep (DP = 52°–59°), and the other one is gentler (DP = 32°–38°). There was thrust motion with a minor left-lateral strike-slip component along the first plane, while the second plane was characterized by thrust motion with a right-lateral strike-slip component. Note that the focal mechanism solutions derived from the moment tensor (NEIC USGS Centroid Moment Solution) and presented in the Quick CMT catalog (United States) are approximately the same as the focal mechanism solution computed at GS RAS. Both nodal planes trend in the same direction as the major axis of the oval-shaped aftershock epicenter area (determined from primary seismically induced fractures, Figs. 11 and 12) and the major axes of oval-shaped high-seismic-intensity isoseismals. Based on seismotectonic data and by analogy with the 2008 Wenchuan earthquake, the gently dipping northwest-trending fault plane that plunges beneath the south-

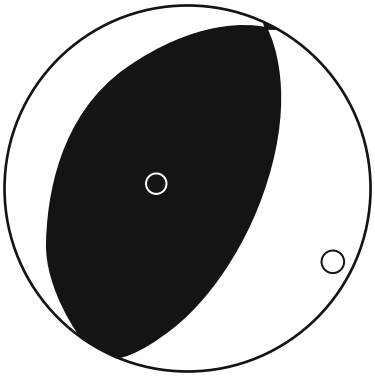

Fig. 13. Focal mechanism solution for 2013 Lushan earthquake on lower hemisphere of stereographic projection (GS RAS).

east slope of the Sinian mountains should be regarded as the main active fault plain. Thus, the earthquake was caused by thrust motion of the northwestern wall of the fault in a southeast direction with a minor left-lateral strike-slip component.

Yushu Earthquake of 2010

An earthquake with a magnitude of 7.1 occurred in Qinghai province (China), near the city of Yushu, on April 14, 2010. More than 2000 people were killed, over 12000 were wounded, and 195 people were missing.

According to the Seismological Bureau of the People's Republic of China, earth tremors were recorded at 07:49 LT, and the hypocenter was at a depth of 10 km (NEIC, GS RAS) in Yushu county of the Tibet Autonomous Region, Qinghai province. The earthquake occurred in the southern part of the Bayan Hara seismotectonic belt. The epicenter was confined to the Grazze–Yushu–Funchuoshan fault zone (Fig. 1).

The main shock resulted in a northwest-striking (315°) zone of primary seismic dislocations, approximately 30 km long (Fig. 14). In terms of morphokinematics, the seismic dislocations were caused by left-lateral strike-slip motion with a minor vertical dip-slip component. There are en echelon systems of shear cracks on the surface, oriented in a west-northwest (280°) direction. The left-lateral strike-slip displacement is up to 1.75 m.

The structure of the seismic rupture zone was studied in a 2-m-deep trench south of the town of Yushu, (Fig. 15). Figure 15a shows a ledge caused by the 2010 earthquake. The left side wall of the trench shows that the fracture plane dips southwestward at an angle of about 70° (Fig. 15c). On the right wall of the trench, the rupture plane dips southwest at an angle of 55° (Fig. 15d). It is observed in the trench that the rupture zone separates different quaternary deposits: dense proluvial and lacustrine loams in the southwestern hanging wall of the fault and coarse-grained alluvial pebble in the footwall. The vertical displacement along the fault indicates that it is a normal fault. The displacement is about 0.5 m.

Thus, from trenching excavation data, it can be concluded that the active Grazze–Yushu–Funchuoshan fault within this segment is of ancient origin.

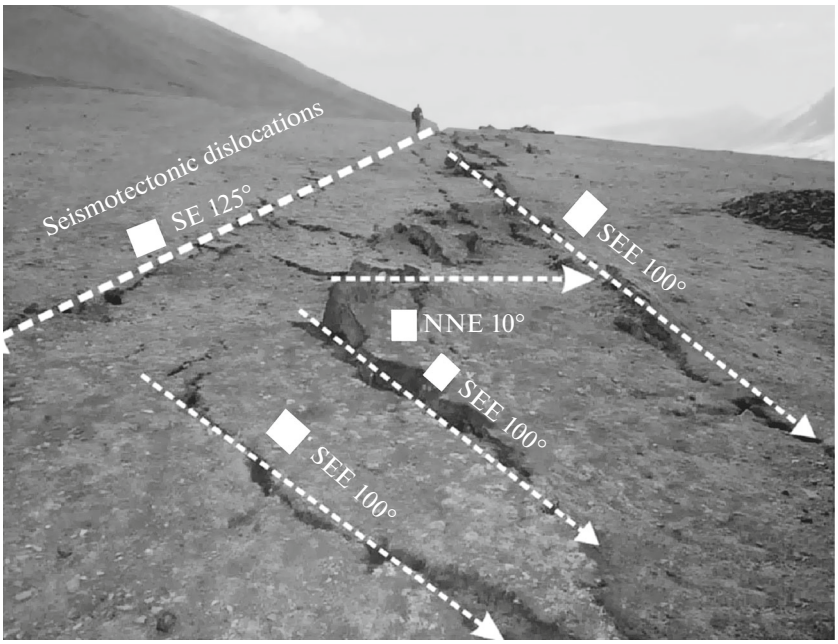

Fig. 14. Seismic rupture caused by 2010 Yushu earthquake (Li Dewei, 2010), south of town of Yushu. View looking west.

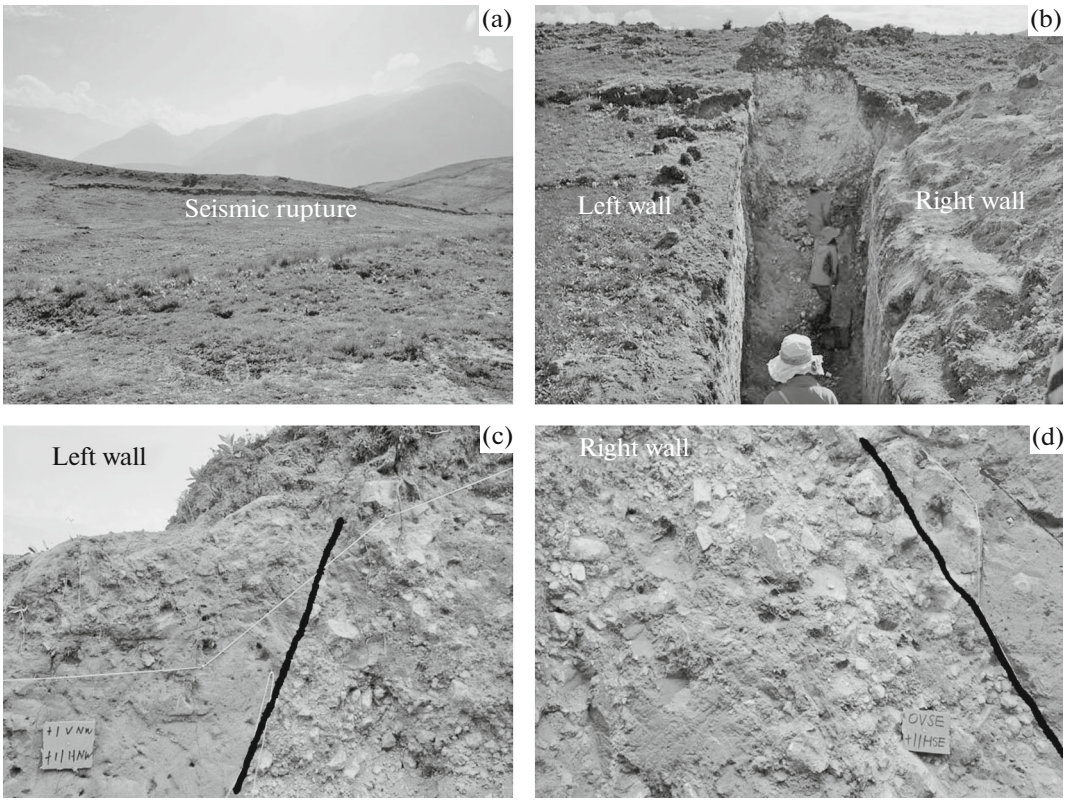

Fig. 15. (a) General view of seismic rupture caused by 2010 Yushu earthquake, south of town of Yushu; panels (b), (c), and (d) show trench across rupture. Photo by Shen Tuo, 2014.

The total amount of displacements along the fault during the Late Quaternary Stage exceeds 2 m.

The focal mechanism solution (Fig. 16) shows that the earthquake resulted from approximately equal tension and compression stresses oriented in the north-south and west-east directions, respectively. One nodal plane strikes northwest and the other one strikes northeast. The northwest trending plane exhibits left-lateral slip along the strike with a subordinate slip downdip. The northeast-trending plane exhibits nearly pure right-lateral slip along strike. A study of the rupture zone on the surface shows that it is the northwest-trending plane that the earthquake source was confined to. This is confirmed by the fact that the major axes of the oval-shaped zones of the epicenters of the foreshock, main shock, and aftershocks are oriented in a northwest-southeast direction (Fig. 17).

Gorkha Earthquake of 2015

A catastrophic earthquake, called the Gorkha earthquake, occurred in Nepal on April 25, 2015. The moment magnitude of the earthquake was $M_W = 7.9$. According to the Emergency Report Service of the Geophysical Survey, Russian Academy of Sciences, the epicenter of the main shock was located at 28.18° N, 84.78° E; the depth of the hypocenter was 15 km.

The earthquake caused about 9000 fatalities; 14500 people were injured. Many buildings were destroyed in Kathmandu, the capital of Nepal,. The earthquake inflicted heavy damage to the historical center of the city. Avalanches on Mt. Everest caused by the earthquake killed 80 climbers. Tremors from the earthquake were felt in China, India, Pakistan, and Bangladesh, where over 100 people lost their lives.

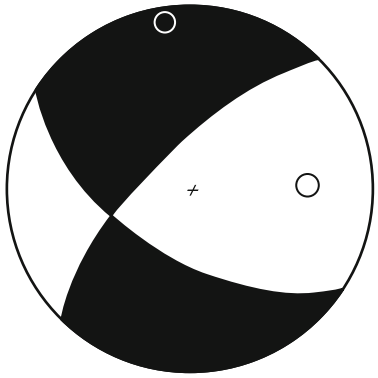

Fig. 16. Stereogram of focal mechanism solution for 2010 Yushu earthquake (data of Geophysical Survey, Russian Academy of Sciences).

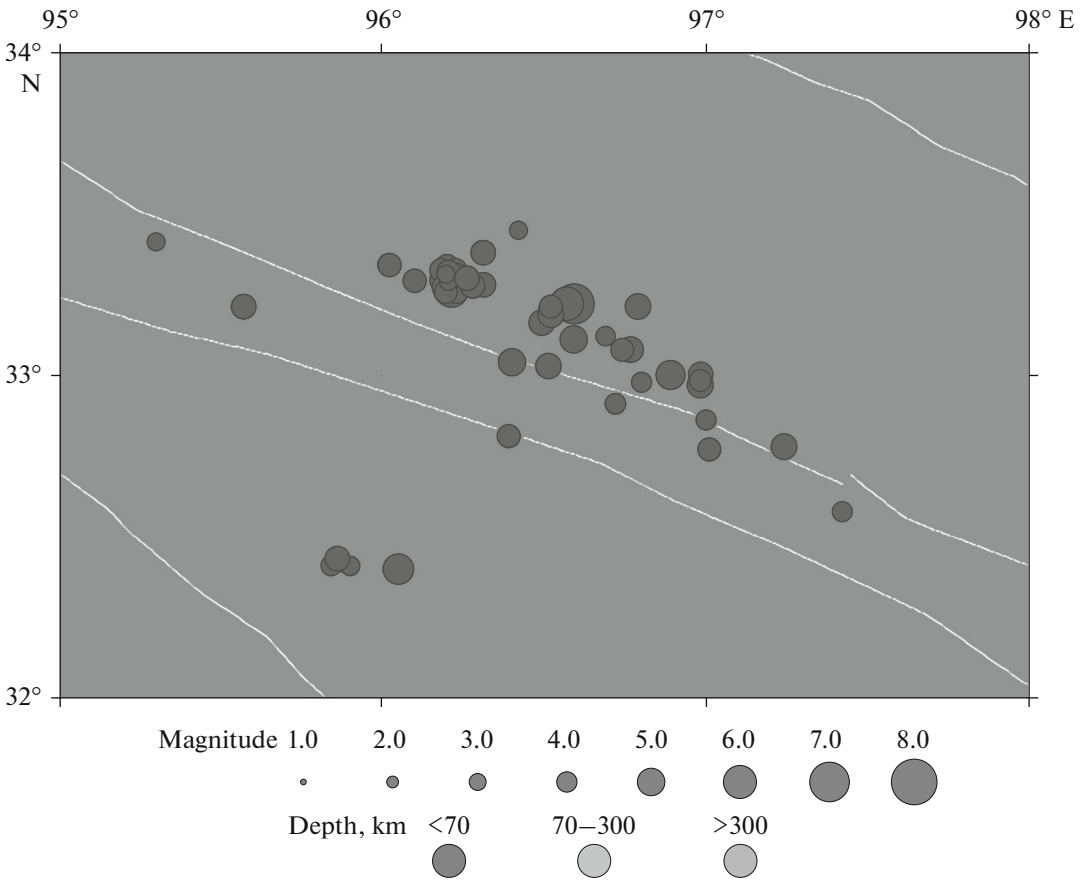

Fig. 17. Epicenters of foreshock, main shock and aftershocks (55 events) of 2010 Yushu earthquake, April 13, 2010, through March 27, 2012 (Sobisevich et al., 2017). Lines show faults.

According to NEIC USGS, the maximum effect of the earthquake was VIII on the Modified Mercalli Intensity (MMI) Scale. Some settlements within the MMI VIII zone experienced MMI IX seismic intensity, but it was impossible to map the MMI IX isoseismals. The MMI VIII area covered the foothills and southern slope of the Great Himalayas; the area had an irregular oval shape: the major axis was oriented in a west-northwest direction, parallel to the strike of the mountain ranges. The MMI VIII area was about 150 km long and 60–70 km wide. The zone of maximum tremors covered Kathmandu and several major cities, such as Panahoti (population 28000), Bharatpur (population 107000), Banepa (population 17000).

No primary seismic dislocations, i.e., surface ruptures caused by the main shock, were observed. In other words, the rupture front did not reach the surface; the earthquake occurred on the so-called blind thrust faults commonly found in the Himalayas. However, there were numerous secondary dislocations. The earthquake caused a large number of landslides and rock falls on steep slopes, vibrational cracks on road surfaces, and snow avalanches in the Great Himalayas. These seismic dislocations were observed on all "appropriate" slopes within the MMI VIII intensity zone (Rogozhin et al., 2016a, 2016b).

American scientists detected 4312 coseismic and postseismic landslips and several landslide-dammed lakes in the epicentral area (Densmore et al., 2015; Kargel et al., 2015).

The instrumental epicenter was in Nepal, 75 km northwest of Kathmandu.

The focal parameters were determined from the distribution of the epicenters of aftershocks that occurred within several months of the main shock. The projection of the Gorkha earthquake source region on the surface is oval in shape, about 160–170 km long and about 70–80 km wide. The depth of most aftershock hypocenters was from 0 to 15 km (Fig. 18).

The nature of motion can be determined from the focal mechanism solution for the main shock. For this, the results of calculations presented in the Global Centroid Moment Tensor database (http://www.globalcmt.org) were used (Fig. 19). The compression axis was oriented in the SSW–NNE direction, across the strike of the Nepalese segment of the Himalayas, and dipped north-northeast at an angle of 30°. The

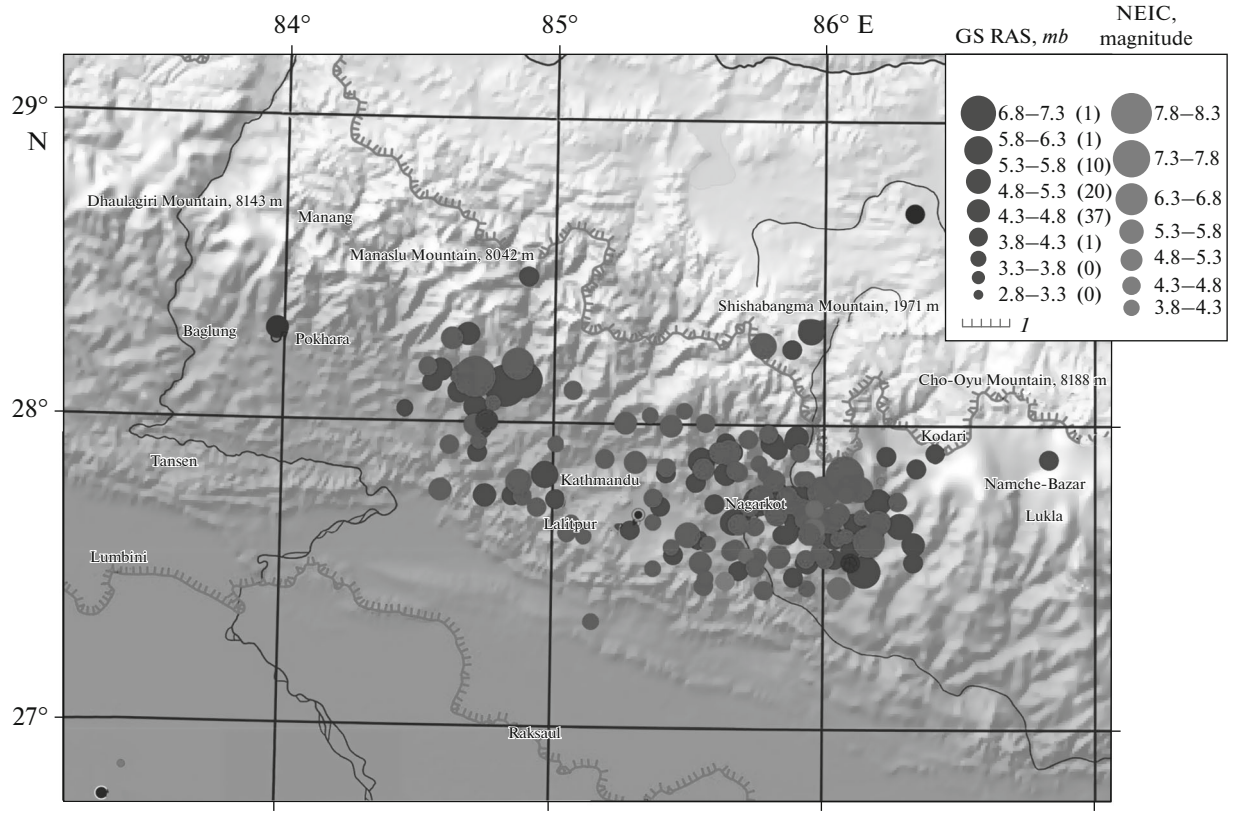

Fig. 18. Epicenters of main shock and aftershocks of April 25, 2015, Gorkha earthquake, as of September 29, 2015. (*I*) Border of Nepal.

tension axis trended approximately in the same direction, dipping south-southeast at an angle of about 60°. One of the alternative faulting planes gently dipped in the north-northeast direction (at an angle of 10°–20°), and the other dipped steeply south-southeast (at an angle of about 70°). The hypocenters of the main shock and most aftershocks were at shallow depths; therefore, the plane gently plunging beneath the Himalayan Fold Mountains was presumably the plane along which movement of rocks predominantly occurred, which was thrust fault movement of the Great Himalayas towards the Lower Himalayas and foothills, with a minor right-lateral strike-slip component.

A source model of the Gorkha earthquake, based on available seismotectonic and seismological data, shows that rock movement occurred along a gently northward-dipping fault plane that originated in the zone of the Main Boundary Thrust of the Himalayas. The main shock resulted in horizontal displacement in the south-southwest direction (about 190°); the displacement varied from 1.5 to 3.5 m depending on location within the earthquake focal region; the vertical displacement reached 2 m (Cheloni, 2015).

EARTHQUAKE ENERGY

Various methods for measuring the magnitude of earthquakes are approximations to the "ideal" energy scale:

$$M = \frac{2}{3}(\log E - 4.8), \quad (1)$$

where E is the earthquake energy in joules.

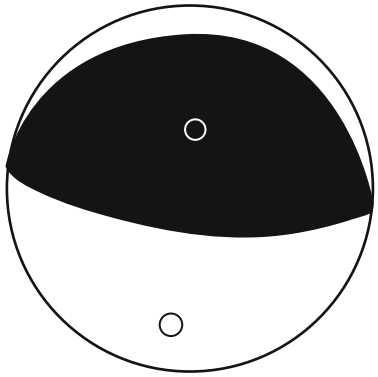

Fig. 19. Stereogram of focal mechanism solution for main shock of April 25, 2015, Gorkha (Nepal) earthquake (http://www.globalcmt.org).

Table 1. Total Seismic Energy Release in Eastern Tibet in 1970–2015

Year	Seismic energy, arb. units	Year	Seismic energy, arb. units
1970	2.67E+14	1993	3.45E+14
1971	1.36E+15	1994	1.57E+14
1972	1.51E+14	1995	2.27E+14
1973	5.1E+16	1996	1.36E+15
1974	2.95E+15	1997	1.28E+15
1975	2.21E+15	1998	2.99E+14
1976	9.98E+15	1999	3.05E+14
1977	1.11E+15	2000	7.97E+14
1978	3.21E+14	2001	8.94E+16
1979	2.1E+14	2002	1.46E+14
1980	2.26E+15	2003	1.14E+15
1981	1.81E+15	2004	5.87E+14
1982	6.51E+14	2005	3.54E+14
1983	1.06E+14	2006	1.1E+14
1984	8.55E+13	2007	1.36E+14
1985	2.82E+14	2008	7.27E+16
1986	1.05E+15	2009	7.37E+14
1987	1.67E+14	2010	3.1E+15
1988	2.15E+15	2011	1.06E+15
1989	4.93E+14	2012	2.67E+14
1990	3.44E+14	2013	2.61E+15
1991	5.52E+14	2014	6.47E+15
1992	9.99E+13	2015	1.42E+17

We used the CENC seismic catalog (http://www.csndmc.ac.cn/newweb/index.jsp) to analyze the seismicity in Tibet and its environs between latitudes 26° and 40° N and between longitudes 77° and 107° E for the period from January 1, 1970, to June 1, 2016. The catalog contains data on 15989 seismic events, the magnitudes of which (*ms*, *ms*7, *ml*, *mb*, and *mB*) were estimated using different seismic waves. We converted all magnitudes to surface-wave magnitudes and then used formula (1) to calculate the energy of every event. On this basis, the total energy released in the region in 1970–2015 was estimated (Table 1).

Figure 20 shows a plot of seismic energy released in the region. Evidently, the period 1973–1975 is characterized by increased seismic activity, which agrees with the worldwide trend in seismic activity in the 1950s through the 1970s (Lutikov and Rogozhin, 2014). Then seismic quiescence ensued for approximately 25 years. Since 2001, there have been three peaks in seismic activity: the 2001 Kunlun earthquake, the 2008 Wenchuan earthquake, and the 2015 Gorkha earthquake. These earthquakes determined the seismic activation in the region at the beginning of the 21st century.

This activation concurs with increased seismic activity throughout the world during this period (Lutikov and Rogozhin, 2014).

TIME-DEPENDENT SEISMICITY MIGRATION IN EASTERN TIBET

Figure 21 shows that the seismic sources moved in the northwest-southeast direction along the faults bounding the Bayan Hara block, gradually weakening in energy. Note that the northern wall of the active fault shifted westward during the Kunlun earthquake, whereas the southern wall moved eastward. The southern massif thus exerted pressure on the northwestern boundary of the Yangtze Platform (the Longmenshan fault zone). And seven years after the Kunlun earthquake, the Wenchuan earthquake occurred, T followed by the Yushu earthquake the source of which was on the west-northwest trending fault bounding the Bayan Hara block in the south-southwest. The Lushan earthquake occurred in 2013; its focal region increased the huge focal region of the Wenchuan earthquake in the southwest, as far as the intersection of the Longmenshan fault system and the Yushu fault.

During the period of increased seismic activity, the deformation of the Bayan Hara lithospheric block

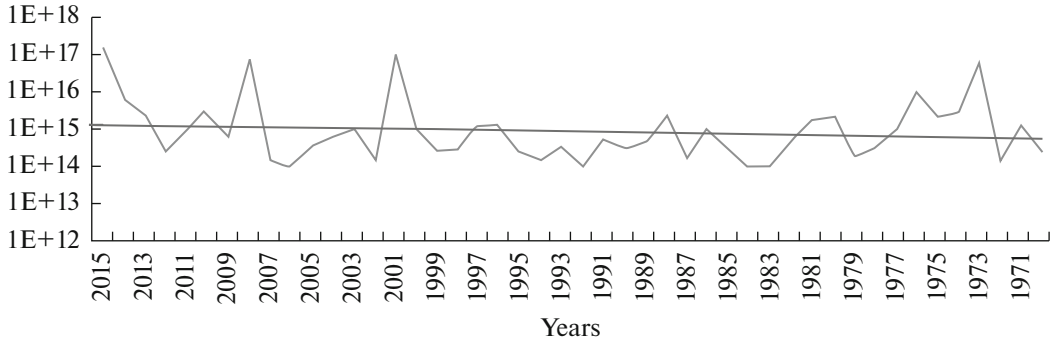

Fig. 20. Total seismic energy released in northeastern Tibet by year (winding line) and general trend of seismic intensity in region (straight line).

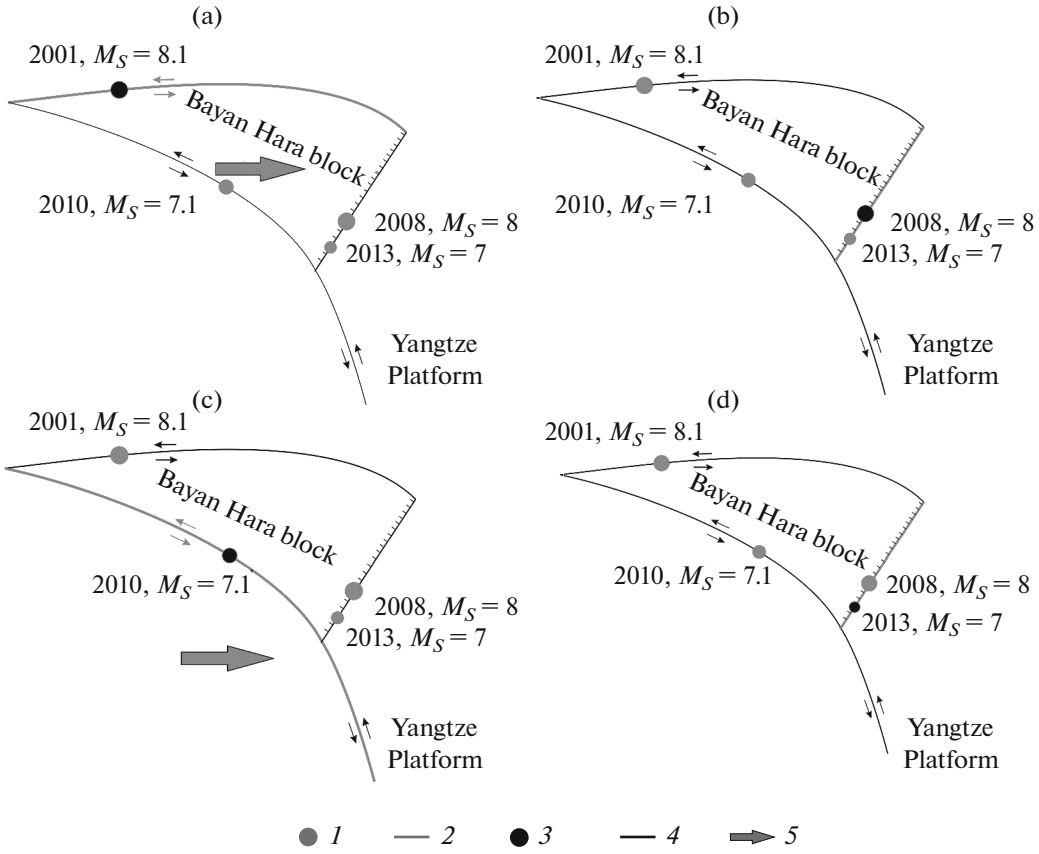

Fig. 21. Scheme of displacements along the faults bounding the Bayan Hara block: (a) November 14, 2001, M_S = 8.1 Kunlun earthquake caused left-lateral strike slip along East Kunlun fault; (b) May 12, 2008, M_S = 8 Wenchuan earthquake caused by right-lateral strike slip and thrust motions along Longmenshan fault zone; (c) April 14, 2010, M_S = 7.1 Yushu earthquake caused by left-lateral strike slip along Grazze–Yushu–Funhuoshan fault; (d) April 20, 2013, M_S = 7 Lushan earthquake caused by right-lateral strike slip and thrust motions along Longmenshan fault. (*1*) Epicenters of earthquakes; (*3*) faults; (*2*) epicenters of active earthquakes at this stage; (*4*) active faults at this stage; (*5*) direction of seismic energy propagation.

along its boundaries resulted from the block being pushed out from the from the central part of the Tibetan Plateau towards the Yangtze Platform. No seismic shocks were observed within the bounds of the block. Therefore, the Bayan Hara block is moving eastward as a single whole (Xu Zhiqin et al., 2011). GPS observations (Wang, 2008) show that there have been hardly any eastward horizontal displacements (which are typical of the eastern part of Tibet) at the boundary with the Yangtze Platform, within which horizontal displacements are negligible. The 2008 and 2013 seismic events were confined to this boundary coinciding with the Longmenshan fault zone.

Figure 22 shows a submeridional plot of the locations of the five strongest earthquakes in central and eastern Tibet and the Himalayas of Nepal in the north-south direction. Clearly, the epicenters of the largest earthquakes in the 21st century are migrating southward with time.

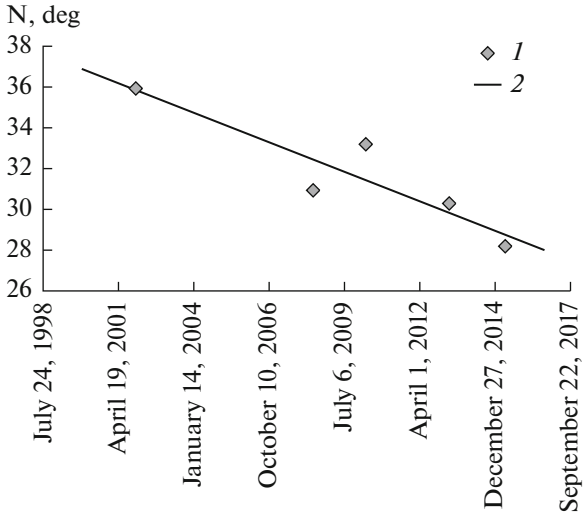

Fig. 22. Spatiotemporal migration of sources of strongest earthquakes in East Tibet and Himalayas of Nepal in 21st century. (*1*) Seismic events; (*2*) general trend.

GEODYNAMIC INTERPRETATION OF THE CAUSE OF INCREASING SEISMIC ACTIVITY IN THE TIBET PLATEAU IN THE 21ST CENTURY

According to the plate tectonics concept, north-dipping subduction of the Hindustan Plate beneath Eurasia consumed the Tethys Ocean Basin 50–60 Ma ago (Molnar, 1978; Tapponnier et al., 1986). Collision of the plates resulted in the formation of the Himalayan fold mountain range. Recently, the Tibetan Plateau has rapidly risen (Dewey, 2005). This cannot be explained solely by the pressure of the colliding Hindustan and Eurasian plates, since no significant changes in the magnitude of upward surface movement in the south-north direction are observed. Also, this viewpoint cannot explain the distribution of the hypocenters of strong earthquakes below the Himalayan belt and the Tibetan Plateau. The hypocenters of virtually all significant seismic events were at depths of 10–35 km. The territory under consideration is a very active seismic zone where earthquakes usually occur in the crust. There are no indications that the seismically active layer is dipping in the direction from the Himalayas to southern and central Tibet.

Recent seismological and geophysical studies have allowed us to assume that seismic activity in Tibet is due to geodynamic processes. Almost all earthquakes below the central and southeastern parts of the Tibetan Plateau in recent decades are characterized by dip-slip focal mechanisms. The compression axis is almost vertical as well, whereas the tension axis is nearly horizontal, oriented in the near west-east direction (Elliott et al., 2010). As mentioned above, the earthquake sources confined to the Bayan Hara lithospheric block bounded by active faults in the north and south are generally characterized by left-lateral strike-slip kinematics, but they exhibit right-lateral strike-slip and thrust movements in the east (the Longmenshan fault zone).

Near north-south-trending dip-slip faults predominate in southern Tibet and western Kunlun, expressed topographically as grabens (Molnar and Tapponnier, 1978). The central and northern parts of Tibet are dominated by north- and northwest-trending rotational faults with downward vertical and left-lateral strike slip offsets; in the east, these faults transform into northeast-trending faults with right-lateral strike-slip and thrust offsets. According to (Milanovskii, 1991), riftogenic grabens oriented in a submeridional direction (N or NNE), are forming in southern Tibet; these structures indicate crustal extension, due to the presence of a large mantle diapir beneath southern and central Tibet. The diapir probably formed as a result of retrograde metamorphism in the lower crust and upper mantle (Artyushkov and Chekhovich, 2014). Such an intrusion is accompanied by the development of submeridional grabens and extension of the upper crust. The existence of the Tibet plume is also confirmed by materials presented in (Xu Zhiqin et al., 2011). Anisotropic seismic tomography of continental China and neighboring regions based on longitudinal waves (Wei Wei et al., 2016) recorded by the Seismological Network of China, the International Seismological Center, and temporary seismic networks deployed across the Tibetan Plateau have provided insights into the deep structure of the upper mantle below this region. Seismotomographic images of the eastern part of the plateau show that the crust (about 50 km thick), characterized by relatively low velocity, is underlain by a high-velocity layer to a depth of 200 km below the southern margins of Tibet and to a depth of 400 km below its central part. The northern boundary of this high-velocity body is almost vertical and traced along the southwestern flank of the Bayan Hara lithospheric block. Below this layer to a depth of 600 km, there is a thick layer characterized by medium and relatively low P-wave velocity. Thus, the upper mantle beneath southern and eastern Tibet is characterized by density inversion: a high-velocity and, therefore, denser layer overlies a lower-velocity, less dense, layer. This may be the cause of the recent uplift of the plateau.

According to data on anisotropy in the high-velocity layer (Wei Wei et al., 2016), there is centrifugal spreading of material from southern Tibet to the north, south, and east. This can also be interpreted as a sign of deep diapirism in the low-velocity layer of the upper mantle beneath the plateau.

CONCLUSIONS

Tibet is one of the most seismically active continental regions in the world. Throughout human history, the strongest earthquakes have been recorded here. The five devastating earthquakes in the eastern and southern parts of the plateau at the beginning of the 21st century are no exception. The energy of each earthquake was estimated from data from the CSN seismic catalog. It was concluded that there was apparent seismic quiescence in Tibet in the 1980s–2000s. The early 2000s were marked by increased seismic activity in the region. The main tremors were confined to the northern and eastern boundaries of the Bayan Hara block located in the northeastern part of the Tibetan Plateau. The strongest destructive earthquake occurred in the Himalayas of Nepal. In other words, the earthquake sources were located around the central and southern parts of eastern Tibet.

Based on spatiotemporal analysis of the distribution of the sources of the strongest earthquakes, it can be assumed that higher levels of seismic activity migrated across Tibet at the beginning of the 21st century. Seismic events moved in the north-south direction with time, surrounding the Bayan Hara block, the eastern part of the plateau at the boundary with the Yangtze Plate and, finally, the Himalayas at the boundary with the Hindustan plate.

This conclusion contradicts the recent concepts of seismicity and modern geodynamics in central Tibet. It was commonly believed that all the energy causing the uplift of the Tibetan Plateau and increasing seismic activity comes from outside, as a result of the Hindustan Plate moving in the south-north direction. Earthquakes have always been considered an important factor in terms of tectonic energy release. In the 21st century, a different pattern has been observed: earthquakes have migrated to the south, encircling eastern Tibet in the north, east, and south. Therefore, in light of the new data, the seismicity of the region may be due rather to other geodynamic reasons than subduction of the Hindustan Plate beneath Tibet.

REFERENCES

Artyushkov, E.V. and Chekhovich, P.A., Mechanisms of recent crustal uplifts in the Phanerozoic and Precambrian fold belts, in *Materialy XLVI Tektonicheskogo soveshchaniya "Tektonika skladchatykh poyasov Evrazii: Skhodstvo, razlichie, kharakternye cherty noveishego goroobrazovaniya, regional'nye obobshcheniya"* ("Tectonics of the Eurasian Fold Belts: Similarities, Differences, Characteristic Features of Recent Orogeny, and Regional Generalization." Proceedings of the XLVI Meeting on Tectonics), Moscow: GEOS, 2014, vol. 1, pp. 3–6.

Burchfiel, B.C., Royden, L.H., van der Hilst, P.O., Hager, B.H., Chen, Z., King, R.W., Li, G., Lu, J., Yao, H., and Kirby, E., A geological and geophysical context for the Wenchuan earthquake of 12 May 2008, Sichuan, People's Republic of China, *GSA Today*, 2008, vol. 18, No. 7, pp. 4–11.

Chandra, U., Seismotectonics of Himalaya, *Current Sci.*, 1992, vol. 62, pp. 40–71.

Cheloni, D., Coseismic slip model of the M 7.8 2015 Nepal earthquake and its M 7.2 aftershock from joint inversion of InSAR and GPS data, 2015. doi 10.13140/RG.2.1.3263.4720

Chen Yun-tai, Xu Li-sheng, and Zhang Yong, Report on the Great Wenchuan earthquake source of May 12, 2008.

Deng Qidong, Gao Xiang, Chen Guihua, et al., Recent tectonic activity of Bayankala fault-block and the Kunlun–Wenchuan earthquake series of the Tibetan Plateau, *Earth Sci. Front.*, 2010, vol. 17, no. 5, pp. 163–178.

Densmore, A., Dijkstra, T., Jordan, C., et al., Nepal: Update on landslide hazard following 12 May 2015 earthquake, 2015. http://ewf.nerc.ac.uk/2015/05/12/nepal-update-on-landslide-hazard-following-12-may-2015-earthquake/. Accessed April 1, 2018.

Dewey, J.F., Orogeny can be very short, *Proc. Natl. Acad. Sci.*, 2005, vol. 102, pp. 15286–15293.

Elliott, J., Walters, R., England, P., Parsons, B., et al. Extension on the Tibetan Plateau: Recent normal faulting measured by InSAR and body wave seismology, *Geophys. J. Int.*, 2010, vol. 183, no. 2, pp. 503–535.

Engdahl, E.R. and Villaseñor, A., Global seismicity: 1900–1999, in *International Handbook of Earthquake and Engineering Seismology*, vol. 81, Pt. A of *International Geophysics*, Lee, W.H.K., Kanamori, H., Jennings, P.C., and Kisslinger, C., Eds., Academic Press, 2002, pp. 665–690. doi https://org/10.1016/S0074-6142(02)80244-3

Fu Bihong, Wang Ping, Kong Ping, Shi Pilong, and Zheng Guodong, *Atlas of Seismological and Geological Disasters Associated with the 12 May 2008, M_S 8.0 Wenchuan Great Earthquake*, *Sichuan, China*, Beijing: Seismol. Press, 2009.

Gansser, A., The morphogenic phase of mountain building, in *Mountain Building Process*, Hsu, K.J., Ed., London: Academic Press, 1982, pp. 221–228.

Geophysical Survey of the Russian Academy of Sciences, Last earthquakes. http://www.ceme.gsras.ru/new/eng/ssd_news.htm. Accessed April 1, 2018.

Global Centroid-Moment-Tensor Project. http://www.globalcmt.org. Accessed April 1, 2018.

Guohua Gu, Wuxing Wang, Yueren Xu, and Wenjun Li, Horizontal crustal movements before the great Wenchuan earthquake obtained from GPS observations in the regional network, *Earthquake Sci.*, 2009, vol. 22, no. 5, pp. 471–478.

Kargel, J.S., Leonard, G.J., Shugar, D.H., et al., Geomorphic and geologic controls of geohazards induced by Nepal's 2015 Gorkha earthquake, *Science*, 2016, vol. 351, no. 6269, pp. 140–149.

Li Dewei, The regularity and mechanism of East Kunlun, Wenchuan and Yushu earthquakes and discussion on genesis and prediction of continental earthquakes, *Earth Sci. Front.*, 2010, vol. 17, no. 5, pp. 179–192.

Liu Yanqiong, Zhao Jisheng, and Liu Peixuan, GPS-based analysis of large earthquakes sequence on active faults near Chuanqing block, *J. Nat. Disasters*, 2015, vol. 4, no. 3, pp. 58–66.

Lombardi, A.M. and Marzocchi, W., Evidence of clustering and nonstationarity in the time distribution of large worldwide earthquakes, *J. Geophys. Res.: Solid Earth*, 2007, vol. 112. doi 10.1029/2006JB004568

Lutikov, A.I. and Rogozhin, E.A., Variations in the intensity of the global seismic process in the 20th and the beginning of the 21st centuries, *Izv., Phys. Solid Earth*, 2014, vol. 50, no. 4, pp. 484–500.

Milanovskii, E.E., *Osnovnye etapy riftogeneza na territorii Kitaya* (Main Stages of Rifting in the Territory of China), Moscow: Nedra, 1991.

Molnar, P. and Tapponnier, P., Active tectonics of Tibet, *J. Geophys. Res.*, 1978, vol. 83, no. B1, pp. 5361–5375.

Pandey, M.R., Tandukar, R.P., Avouac, J.P., Vergne, J., and Heritier, T.H., Seismotectonics of the Nepal Himalaya from local seismic network, *J. Asian Earth Sci.*, 1999, vol. 17, pp. 703–712.

Ran, Y.K., Chen, L.C., Chen, G.H., et al. Primary analyses of in-situ recurrence of large earthquake along seismogenic fault of the $M_S = 8.0$ Wenchuan earthquake, *Seismol. Geol.*, 2008, vol. 30, No. 3, pp. 630–643.

Rogozhin, E.A., Lutikov, A.I., and Tuo Shen, Tectonic position and geological and seismic manifestations of the Gorkha earthquake of April 25, 2015, in Nepal, *Geotectonics*, 2016a, vol. 50, no. 5, pp. 522–533.

Rogozhin, E.A., Lutikov, A.I., Sobisevich, L.E., To Shen, and Kanonidi, K.Kh., The Gorkha earthquake of April 25, 2015 in Nepal: Tectonic position, aftershock process, and possibilities of forecasting the evolution of seismic situation, *Izv., Phys. Solid Earth*, 2016b, vol. 52, no. 4, pp. 534–549.

Sobisevich, L.E., Rogozhin, E.A., Sobisevich, A.L., To Shen, and Ziao Liu, Instrumental observations of geomagnetic disturbances prior to seismic evens in several regions of China, *Seism. Instrum.*, 2017, vol. 53, no. 1, pp. 28–45.

Tapponnier, P., Peltzer, G., and Armijo, R., On the mechanics of the collision between India and Asia*, in Collision Tectonics,* Vol. 19 of *Geol. Soc.* London, Spec. Publ., Ed. by Coward, M.P. and Ries, A.C. (London, 1986), pp. 115–157.

USGS Earthquake Hazards Program. http://earthquake.usgs.gov. Accessed April 1, 2018.

USGS, Search earthquake catalog. http://earthquake.usgs.gov/earthquakes/search/. Accessed April 1, 2018.

Valdiya, K.S., The two intracrustal boundary thrusts of the Himalaya, *Tectonophysics*, 1980, vol. 66, pp. 323–348.

Valdiya, K.S., Tectonics and evolution of the central sector of the Himalaya, *Philos. Trans. R. Soc., A*, 1988, vol. 326, pp. 151–175.

Van der Woerd, J., Klinger, Y., Tapponnier, P., Xu, X., Chen, W., Ma, W., and King, G., Coseismic offsets and style of surface ruptures of the 2001 Mw = 7.8 Kokoxili earthquake (Northern Tibet), *EGS-AGU-EUG Joint Assembly, Nice, France*, 2003, Abstr. ID 11151.

Wang, Y.Z., Wang, E.N., Shen, Z.K., et al. GPS-constrained in version of present-day slip rates along major faults of the Sichuan–Yunnan region, *Sci. China, Ser. D: Earth Sci.*, 2008, vol. 51, no. 9, pp. 1267–1283.

Wei Wei, Dapeng Zhao, Xu Jiandong, Zhou Bengang, and Yaolin Shi, Depth variations of P-wave azimuthal anisotropy beneath Mainland China, *Sci. Rep.*, 2016, vol. 6. doi doi 10.1038/srep29614

Xu Zhiqin, Yang Jingsui, Li Haibing, Ji Shaocheng, Zhang Zeming, and Liu Yan, On the tectonics of the India–Asia collision, *Acta Geol. Sin.*, 2011, vol. 85, no. 1, pp. 1–33.

Xu Xiwei, Chen Guihua, Yu Guihua, et al., Seismogenic structure of Lushan earthquake and its relationship with Wenchuan earthquake, *Earth Sci. Front.*, 2013, vol. 20, no. 3, pp. 11–20.

Xu Xi-wei, Wen Xue-ze, Ye Jian-qing, et al., The M_S = 8.0 Wenchuan earthquake surface ruptures and its seismogenic structure, *Seismol. Geol.*, 2008, vol. 30, no. 3, pp. 597–629.

Yan Xue, Jie Liu, Shirong Mei, and Zhiping Song, Characteristics of seismic activity before the M_S = 8.0 Wenchuan earthquake, *Earthquake Sci.*, 2009, vol. 22, pp. 519–529.

Translated by B. Shubik